

# Zinc-induced mirror disordering for high-speed 850 nm VCSEL operated at 40 GB/s OOK

Chun-Yen Peng<sup>1</sup>, Cheng-Han Wu<sup>1</sup>, Shan-Fong Leong<sup>1</sup>, and Chao-Hsin Wu<sup>1,2</sup>

<sup>1</sup>Graduate Institute of Photonics and Optoelectronics

<sup>2</sup>Graduate Institute of Electronics Engineering

National Taiwan University

1, Roosevelt Road, Sec.4, Taipei, 106 Taiwan

Corresponding Author E-mail address: chaohsinwu@ntu.edu.tw

**Keywords:** High speed VCSEL, Zinc-induced disordering, 20 GHz VCSEL

## Abstract

Through the zinc-induced disordering of mirror resistance, vertical-cavity surface-emitting lasers (VCSEL) with 22.5 GHz optical 3dB bandwidth and 40 Gbps on-off-key (OOK) transmission are successfully achieved. VCSELs exhibit lower threshold current and higher optical bandwidth after applying 1.5  $\mu\text{m}$  depth of zinc-induced disordering. With 20-ohm series-resistance reduction, the maximum optical bandwidth can be effectively improved from 19.7 to 22.5 GHz. In addition, the threshold current can be simultaneously reduced from 0.29 to 0.22 mA.

## INTRODUCTION

Since the first pn junction based vertical-cavity surface-emitting lasers (VCSEL) demonstrated by Iga, et al. in 1979 [1] and the development of oxidation technology [2, 3], oxide-confined VCSEL applications have become increasingly popular due to the features of low power consumption and high optical bandwidth. Different techniques have been proposed to improve the threshold current, slope efficiency and optical bandwidth, such as band-gap engineering [4], reduction of parasitic capacitance [5], differential gain enhancement [6], and oxide-relief process [7]. However, these are usually accompanied by yield problems due to high lattice stress of the quantum well or physical damage induced from processing. Hence, in this report we provide an improved process to incorporate zinc disordering of the semiconductor mirror of VCSELs to further reduce parasitic resistance and improve device DC and RF performance.

Firstly, VCSELs with and without a zinc-disordering process are compared for the same epitaxial structure. Threshold currents and optical outputs are improved greatly in the VCSEL with 1.5  $\mu\text{m}$  depth zinc-induced disordering. Differential resistance is characterized by small-signal analysis. Series resistance of the distributed-Bragg-reflector (DBR) mirror reduces from 55 to 35 ohm, and the highest optical bandwidth is 22.5 GHz after applying 1.5  $\mu\text{m}$  zinc-induced disordering. Finally, the zinc-induced VCSEL is tested under a 40 Gbps transmission system, demonstrating its stability by direct-modulation.

## VCSEL FABRICATION AND DC CHARACTERISTICS

The epitaxial material was grown on a semi-insulating GaAs substrate by MOCVD at LandMark Corporation, Taiwan. The optical cavity is formed by top and bottom DBR mirrors in the vertical direction. The active region consists of three  $\text{In}_{0.08}\text{Ga}_{0.92}\text{As}/\text{Al}_{0.35}\text{Ga}_{0.65}\text{As}$  quantum wells (QWs) in a  $1.5\text{-}\lambda$  cavity, and the DBR mirrors are composed of  $\text{Al}_{0.9}\text{Ga}_{0.1}\text{As}/\text{Al}_{0.12}\text{Ga}_{0.88}\text{As}$ .

The fabrication starts with two types of p-metal processing. The first process is Au/Zn metal evaporation for surface diffusion. A high doping concentration in the surface layer can be formed under a low annealing temperature ( $< 400^\circ\text{C}$ ). The second process is impurity-induced disordering by a zinc source. Figure 1(a) shows the cross-section view of a zinc-induced disordering interface with a 1.5  $\mu\text{m}$  depth. The dashed line clearly points out the depth of zinc-induced disordering. A homogenous disordering interface is created by high temperature ( $\sim 600^\circ\text{C}$ ) annealing in a furnace for 12 min, providing a low resistance path of current injection. VCSELs with the two different p-metal processes, are fabricated together with the same process for the remaining steps. The oxidation aperture ( $\sim 5 \mu\text{m}$ ) is confirmed by an infrared optical microscope as shown in Fig. 1(b). In this way, the optical output of VCSELs with different zinc-induced disordering depths can be compared.

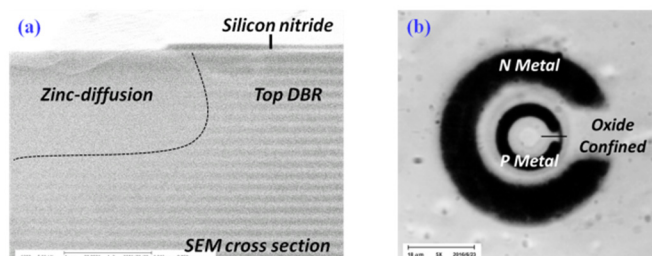


Fig. 1. (a) SEM of p-type DBR after zinc-induced disordering and (b) Top-view of a VCSEL taken by infrared optical microscope.

A schematic of an impurity-induced VCSEL is shown in Fig. 2. The oxidation aperture,  $W_0$ , is 5  $\mu\text{m}$ .  $W_z$  is 10.5  $\mu\text{m}$  corresponding to the open window of impurity-induced disordering.  $H_z$  is 1.5  $\mu\text{m}$  corresponding to the depth of

impurity-induced disordering. The schematic shows that the open window of impurity-induced disordering is larger than the oxidation aperture. Therefore, we can ensure that the mirror reflection will not be affected by the disordering process. Fig. 3(a) shows L-I curves for the two different processes at 25 °C. When the diffusion depth increases from the surface to 1.5  $\mu\text{m}$ , the threshold current reduces from 0.29 to 0.22 mA, and the slope efficiency improves from 0.495 to 0.559 mW/mA. At the same time, the differential resistance decreases from 133.5 to 113.6 ohm when operation current is 5 mA as shown in Fig. 3(b). Additionally, the maximum optical power of the impurity-induced VCSEL is 2.31 mW as compared to 2.28 mW for the VCSEL with Au/Zn metal. The similar optical powers demonstrate that the impurity-induced process doesn't affect the optical output.

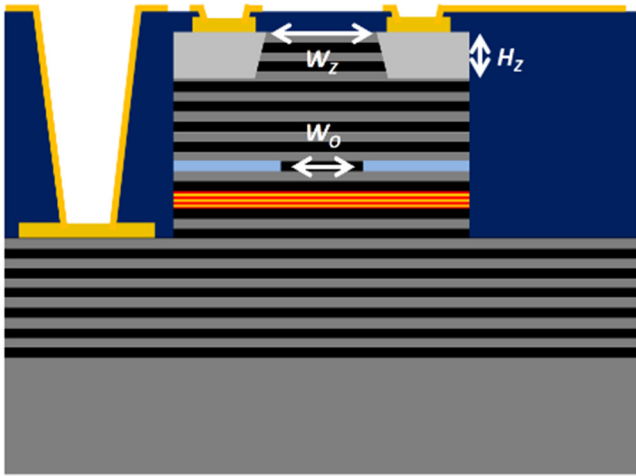


Fig. 2. Schematic of an impurity-induced VCSEL

## RF CHARACTERISTIC AND TRANSMISSION RESULTS

In order to investigate the effects of zinc-induced disordering, S-parameter ( $S_{11}$ ) measurements were used for parameter extraction to construct a small-signal circuit as shown in Fig. 4. The series-resistance drops from 55 to 35 ohm, and the electrical bandwidth of the small-signal circuit increases from 6.4 to 14.71 GHz after zinc-induced disordering.

The small reflection can be directly quantified from  $S_{11}$ . Therefore, the magnitude of  $S_{11}$  and optical response are plotted together in Fig. 5, further emphasizing the advantage of impurity-induced disordering. When the microwave signal is at low frequency, the overall reflection is determined by the differential resistance. Hence, the magnitude of the impurity-induced VCSEL is lower than that of the metal-diffused VCSEL due to the higher doping in the DBR mirror. When the microwave signal increases toward high frequency, the overall reflection is determined by the injection efficiency. Hence, the reflection magnitude will be further reduced compared to that of the metal-diffused VCSEL. The overall bandwidth also responds to this effect. The impurity-induced

VCSEL shows improvement of optical bandwidth from 19.7 to 22.5 GHz.

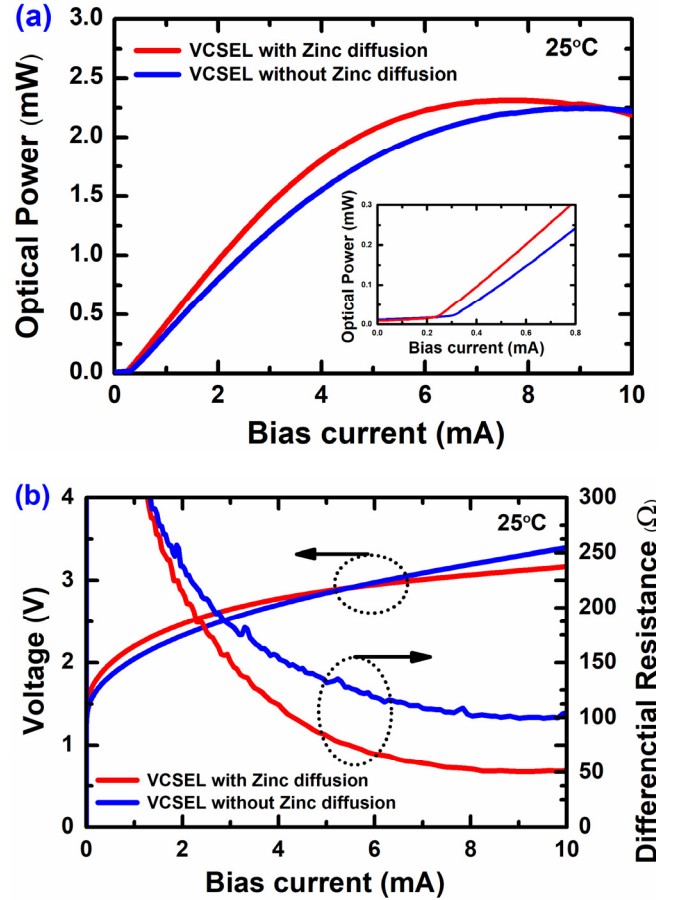


Fig. 3. (a) Light versus current and (b) voltage-current-differential resistance of the VCSELs. The VCSEL with only surface diffusion is the blue line and the VCSEL with 1.5  $\mu\text{m}$  zinc-induced disordering is the red line.

The K factor and D factor are shown in Fig. 6. We have labeled the impurity-induced VCSEL as ZD (zinc-diffused), and the other one as CV (conventional). We use the K and D factor as an efficiency index. The K factor is the slope of the damping factor versus resonant frequency,  $f_r$ . The damping factor can be expressed as  $\gamma = Kf_r^2 + \gamma_0$ . A larger damping factor mainly comes from the self-heating effect of lasers. Hence, a smaller K-factor implies a smaller thermal limitation of lasers, which also provides lasers with larger bandwidth. The D factor is proportional to the resonant frequency, which can be expressed as  $f_r = D\sqrt{I - I_{th}}$ . This factor can more directly represent the energy efficiency of VCSEL. A larger D-factor can drive lasers with larger bandwidth through a lower current. When diffusion depth increases from surface to 1.5  $\mu\text{m}$ , the K factor improves from 0.27 to 0.24 ns, and the D factor increases from 6.0 to 8.5 GHz/(mA)<sup>1/2</sup>. The extraction results demonstrate that the optical bandwidth is improved with zinc-diffusion. Both of them verify that the

zinc-diffusion VCSEL has more efficiency on the issues of bandwidth enhancement.

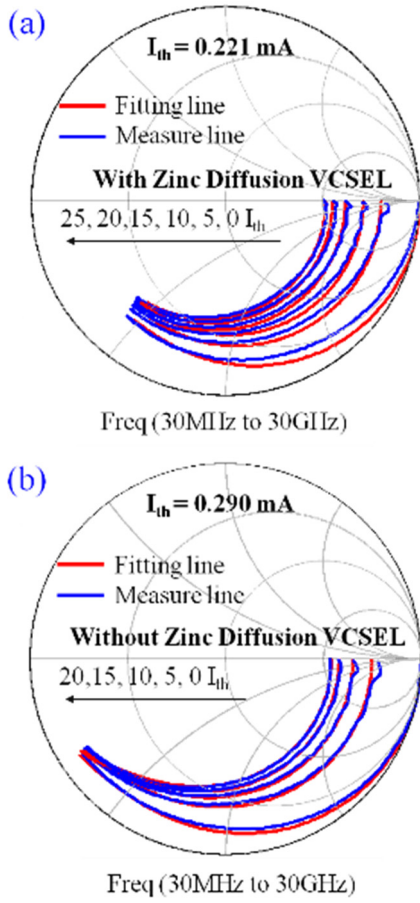


Fig. 4. S-parameter measurements and fitting results for (a) the VCSEL with only surface diffusion and (b) the VCSEL with zinc-induced disordering diffusion. The measurement current starts from 0 mA to the maximum bandwidth current.

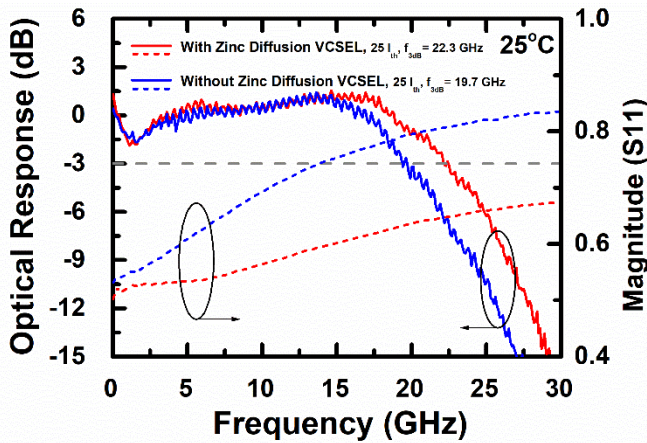


Fig. 5. Optical frequency response and  $S_{11}$  when the VCSELs are biased at maximum bandwidth.

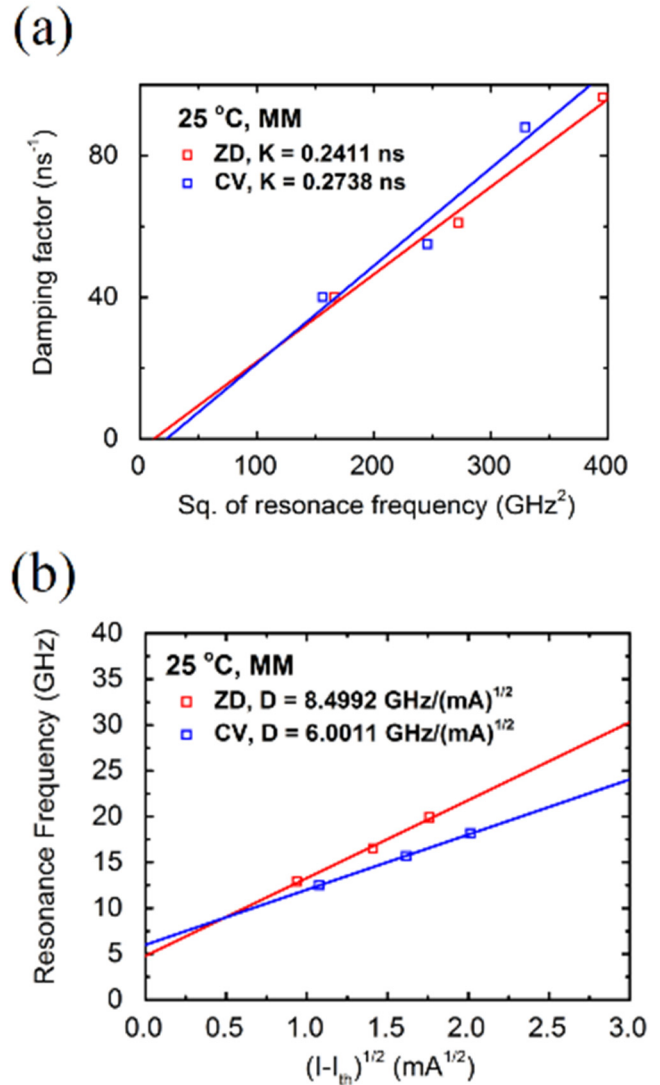


Fig. 6. The extraction of (a) K factor and (b) D factor from the small-signal model.

After small-signal analysis, the VCSEL with zinc-induced disordering is applied to 40 Gbps transmission by on-off key format. The testing bit sequence is non-return-to-zero  $2^7-1$  pseudorandom binary sequence, and the confidence level of error free is higher than 95% in these measurements. Additionally, the OM4 optical fiber is used in this experiment, which offers an Effective Modal Bandwidth of 4700 MHz-km. This is the latest commercial fiber in multimode fiber option. The series of OM (“Optical Multimode”) provide a solution for short-range optical-communication. In order to reduce the dispersion problem, such as different mode delay, a parabolic manner was employed in OM3 and OM4 fiber, which can reduce the arrived time-difference of modes during the optical transmission. The OM4 fiber further enhances the quality of manufacturing process. An extremely precise refractive index profile provides an improved Effective Modal Bandwidth. Hence, the OM4 can also be called

OM3/550 fiber, meaning that 10 Gb/s can be transmitted up to 550 m by 850 nm-VCSELs. Figure 7 shows the 40 Gbps optical eye passing 3m (back to back) and 100m OM4 optical fiber when the VCSEL is under 4 mA bias. The VCSEL is able to show open eyes for both cases. Then we tested the bit-error-rate (BER) of the VCSEL versus received optical under the same operation conditions. The testing results show that two different transmission lengths can pass the error-free testing (BER less than  $10^{-12}$ ), and the power penalty is only 2.2 dBm due to the advantage of the small-size aperture. From the DC and RF measurements, the zinc-induced disordering VCSEL shows lower threshold and higher optical bandwidth. Furthermore, it also displays a high-stability after BER testing with high confidence-level condition, which provides an improved solution for device characteristics.

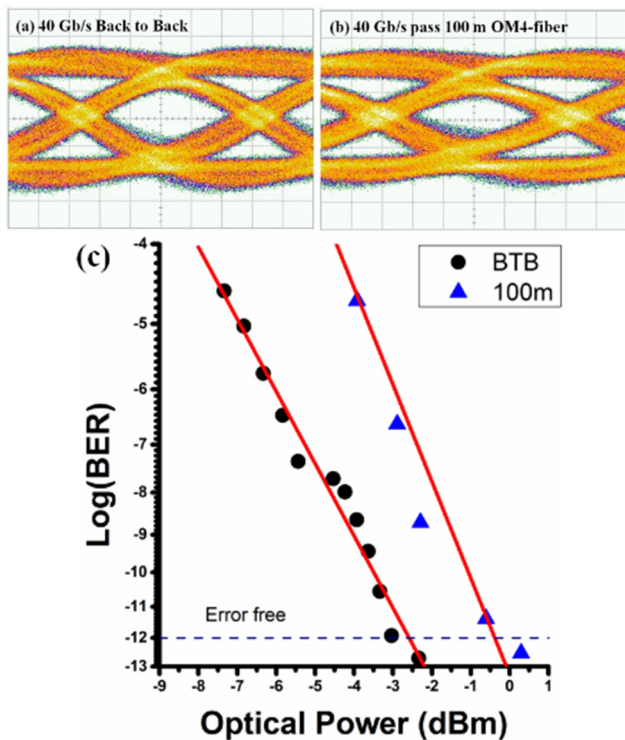


Fig. 7. Eye diagrams of the VCSELs at 40 Gbps OOK transmission for the zinc-induced VCSEL under (a) 3m optical fiber and (b) 100m optical fiber. BER vs. received optical power measurement is shown in (c).

## CONCLUSIONS

With zinc-induced disordering, 40 Gbps data transmission can be achieved through 100m optical fiber. The VCSEL with zinc-induced disordering has lower threshold current, lower p-type mirror resistance, and higher optical bandwidth. This process successfully provides a simple way toward high-speed VCSELs.

## ACKNOWLEDGEMENTS

The authors are thankful for the support of Ministry of Science and Technology of Taiwan (ROC) under Grant Nos. MOST 106-2218-E-005-001, MOST 106-2622-E-002-023-CC2, MOST 105-2628-E-002-007-MY3, MOST 104-2218-E-005-004, and MOST 106-2923-E-002-006-MY3. The authors are thankful for the measurement technical support from Curtis Y. Wang, Junyi Qiu, Prof. Milton Feng and Prof. Nick Holonyak, Jr. at University of Illinois at Urbana-Champaign.

## REFERENCES

- [1] H. Soda, K. Iga, et al., "GaInAsP/InP surface emitting injection lasers," *Japan. J. Appl. Phys.*, vol. 18, pp. 2329-2330, Dec. 1979..
- [2] J. M. Dallesasse, N. Holonyak, Jr. et al, "Hydrolyzation oxidation of AlGaAs-AlAs-GaAs quantum well heterostructures and superlattices," *Appl. Phys. Lett.*, vol. 57, pp. 2844-2846, 1990
- [3] D. L. Huffaker, D. G. Deppe, et al., "Nativeoxide defined ring contact for low-threshold vertical-cavity lasers," *Appl. Phys. Lett.*, vol. 65, pp. 97-99, 1994..
- [4] K. Kojima, et al., "Reduction of p-doped mirror electrical resistance of GaAs/AlGaAs vertical-cavity surface-emitting lasers by delta doping," *Electron. Lett.*, vol. 29, pp. 1771-1772, 1993.
- [5] M. Azuchi, F. Koyama, et al., "Multioxide layer vertical-cavity surface-emitting lasers with improved modulation bandwidth," in *Proc. Conference on Lasers and Electro-Optics*, vol. 1, 2003, p. 163, paper W2B-(2)-6.
- [6] S. B. Healy, A. Joel, et al., "Active region design for high speed 850 nm VCSELs," *IEEE J. Quantum Electron.*, vol. 46, no. 4, pp. 506-512, Apr. 2010.
- [7] J. Shi, et al., "Oxide-relief vertical-cavity surface emitting lasers with extremely high data-rate/power-dissipation ratios," in *Proc. Opt. Fiber Commun. Conf. Expo./Nat. Fiber Opt. Eng. Conf.*, Los Angeles, CA, USA, 2011, pp. 1-3.

## ACRONYMS

VCSEL: vertical-cavity surface-emitting lasers  
 DBR: distributed-Bragg-reflector  
 QWs: quantum wells  
 OOK: on-off-key  
 MOCVD: Metal-Organic Chemical Vapor Deposition  
 BER: bit-error-ratio